Partial Oxidation of Propylene Catalyzed by VO_3 Clusters: A Density Functional Theory Study

Zhe-Chen Wang,[†,‡] Wei Xue,[†,‡] Yan-Ping Ma,[†] Xun-Lei Ding,[†] Sheng-Gui He,*[,†] Feng Dong,[§,⊥] Scott Heinbuch,[||,⊥] Jorge J. Rocca,[||,⊥] and Elliot R. Bernstein[§,⊥]

Beijing National Laboratory for Molecular Sciences, State Key Laboratory for Structural Chemistry of Unstable and Stable Species, Institute of Chemistry, Chinese Academy of Sciences, Zhongguancun, Haidian, Beijing 100080, P. R. China, Graduate School of Chinese Academy of Sciences, Beijing 100039, P. R. China, Department of Chemistry, Colorado State University, Fort Collins, Colorado 80523-1872, Department of Electrical and Computer Engineering, Colorado State University, Fort Collins, Colorado 80523-1373, and NSF ERC for Extreme Ultraviolet Science and Technology

Received: December 8, 2007; Revised Manuscript Received: April 12, 2008

Density functional theory (DFT) calculations are carried out to investigate partial oxidation of propylene over neutral VO_3 clusters. C=C bond cleavage products $CH_3CHO + VO_2CH_2$ and $HCHO + VO_2CHCH_3$ can be formed overall barrierlessly from the reaction of propylene with VO_3 at room temperature. Formation of hydrogen transfer products $H_2O + VO_2C_3H_4$, $CH_2{=}CHCHO + VO_2H_2$, $CH_3CH_2CHO + VO_2$, and $(CH_3)_2CO + VO_2$ is subject to tiny (0.01 eV) or small (0.06 eV, 0.19 eV) overall free energy barriers, although their formation is thermodynamically more favorable than the formation of C=C bond cleavage products. These DFT results are in agreement with recent experimental observations. VO_3 regeneration processes at room temperature are also investigated through reaction of O_2 with the C=C bond cleavage products VO_2CH_2 and VO_2CHCH_3. The following barrierless reaction channels are identified: $VO_2CH_2 + O_2 \rightarrow VO_3 + CH_2O$; $VO_2CH_2 + O_2 \rightarrow VO_3C + H_2O$, $VO_3C + O_2 \rightarrow VO_3 + CO_2$; $VO_2CHCH_3 + O_2 \rightarrow VO_3 + CH_3CHO$; and $VO_2CHCH_3 + O_2 \rightarrow VO_3C + CH_3OH$, $VO_3C + O_2 \rightarrow VO_3 + CO_2$. The kinetically most favorable reaction products are CH_3CHO, H_2O, and CO_2 in the gas phase model catalytic cycles. The results parallel similar behavior in the selective oxidation of propylene over condensed phase V_2O_5/SiO_2 catalysts.

1. Introduction

Vanadium oxides are an important class of heterogeneous catalysts used both in industry and in the laboratory.[1–3] The well-known industrial processes facilitated by vanadium oxide based catalysts include oxidation of SO_2 to SO_3 in the production of sulfuric acid, selective reduction of NO_x with NH_3 for pollution control, selective oxidation of hydrocarbons in the production of more expensive and useful chemicals, and so forth. To interpret these important processes at a molecular, mechanistic level, efforts have been devoted to investigate the chemistry (bonding, structural, and reactivity properties, etc.) of vanadium oxide clusters in the gas phase by both experimental[4–8] and theorical[7–12] means. On the other hand, discovery of new and interesting chemistry of vanadium oxide clusters would finally shed light on design, synthesis, and more effective use of practical catalysts.

The chemistry of neutral vanadium oxide clusters in the gas phase is not well studied experimentally due to difficulties in detection of these neutral metal oxide clusters without fragmentation during multi-photon or electron-impact ionization processes. Single photon ionization through radiation of vacuum ultraviolet and soft X-ray lasers has been effectively employed recently to detect neutral transition metal oxide and sulfide clusters without fragmentation,[13] and the reactivity of neutral vanadium oxide clusters toward C_2 hydrocarbons has been successfully studied.[14] One of the interesting chemistries identified is that $(V_2O_5)_nVO_3 + C_2H_4 \rightarrow (V_2O_5)_nVO_2CH_2 + CH_2O$ occurs under near room temperature conditions, for $n = 0$, 1, and 2. This C=C double bond cleavage reaction is not found in the reaction of cationic vanadium oxide clusters with ethylene. In contrast, a set of oxygen transfer reactions are identified for cationic species: $(V_2O_5)_n^+ + C_2H_4 \rightarrow (V_2O_5)_{n-1}V_2O_4^+ + CH_3CHO$, where $n = 1$, 2, and 3.[6,7] On the basis of density functional theory (DFT) calculations for the neutral VO_3 cluster, the oxygen transfer reaction channel ($VO_3 + C_2H_4 \rightarrow VO_2 + CH_3CHO$) is thermodynamically more favorable than the C=C bond cleavage channel; however, formation of CH_3CHO is kinetically less favorable at room temperature than formation of HCHO due to a higher overall reaction barrier.

The mechanism of the reaction of $(V_2O_5)_nVO_3$ with C_2H_4 is interesting in that the reaction kinetics and the reaction dynamics play opposite roles. This is generally of fundamental importance in selective oxidation of hydrocarbons because formation of unwanted CO_2 and H_2O are usually thermodynamically most favorable. In this work, DFT calculations are employed to investigate the reaction of VO_3 with propylene (C_3H_6), to explore the generality of double bond cleavage of alkenes over VO_3. We anticipate that the additional methyl group of propylene will result in different chemistry for $VO_3 + C_3H_6$ than that found for $VO_3 + C_2H_4$. Moreover, to generate a complete model catalytic cycle, reactions of O_2 with some kinetically allowed products will be considered to regenerate VO_3.

* Author to whom correspondence should be addressed. E-mail: shengguihe@iccas.ac.cn. Phone: 86-10-62536990. Fax: 86-10-62559373.
† Institute of Chemistry, Chinese Academy of Sciences.
‡ Graduate School of Chinese Academy of Sciences.
§ Department of Chemistry, Colorado State University.
⊥ NSF ERC for Extreme Ultraviolet Science and Technology.
|| Department of Electrical and Computer Engineering, Colorado State University.

10.1021/jp7115774 CCC: $40.75
Published on Web 06/06/2008

In the chemical industry, selective oxidation of propylene is particularly important.[15,16] The selective oxidation of propylene over vanadium oxide catalysts supported (Al_2O_3, SiO_2, TiO_2, and Nb_2O_5, etc.)[16–18] or unsupported[19] has been extensively investigated. Products formed with high selectivity are acrolein (CH_2CHCHO) over V_2O_5/Nb_2O_5,[17] acetone [$(CH_3)_2CO$] over V_2O_5/TiO_2,[16] acetaldehyde (CH_3CHO) over V_2O_5/SiO_2,[18] acetaldehyde and acetic acid (CH_3COOH) over $V_2O_5-MoO_3$,[19] and others. The mechanisms for the formation of C=C bond scission products, such as acetaldehyde is not well explored. Ruszel et al.[18] suggest that partial degradation of propylene over supported vanadium oxide catalysts may be considered as an electrophilic surface oxygen species O_2^- or O^- adding to a C=C double bond through the formation of peroxo or oxo intermediates which can decompose by breaking a C−C bond.

To address catalytic mechanisms involving vanadium oxides, considerable efforts have been devoted to determining the structures of catalytically active sites on the supports. Surface monovanadium species are generally accepted to have the structure $O{=}V{-}(O{-}X)_3$ (pyramid model), in which X is an atom (such as Si, Ti, . . .) in the support;[3,20] however, some recent experimental and theoretical studies suggest that the species should have the structure $O{=}V(=O_2){-}O{-}X$ (umbrella model).[21] The structures of the monovanadium sites will be more complicated if surface acidity (hydrogen species) is considered.[22] Evidence indicates that structures of catalytically active sites are dynamic and some reactive intermediates do not live long enough to be captured by available experimental (mainly spectroscopic) techniques.[17] VO_3 has a structure similar to that of the umbrella model surface monovanadium species. VO_3 may also serve as a model for a reactive surface intermediate. Thus VO_3 clusters can serve as a model catalyst to interpret possible surface chemistry and reactive species.

2. Computational Details

DFT calculations using the Gaussian 03 program[23] are employed to study reactions of VO_3 with C_3H_6 and reactions of the kinetically allowed products from $VO_3 + C_3H_6$ with O_2 to regenerate VO_3. The DFT calculations involve geometry optimization of various reaction intermediates and transition states. Transition state optimizations are performed by using either the Berny algorithm[24] or the synchronous transit-guided quasi-Newton (STQN) method.[25,26] For most cases, initial guess structure of the transition state is obtained through relaxed potential energy surface (PES) scans using an appropriate internal coordinate. For a few complicated cases, the initial structure is obtained by using the multi-coordinate driven method[27] that determines the relaxed PES in terms of more than one active internal coordinate. Vibrational frequencies are calculated to check that the reaction intermediates have all positive frequencies and species in the transition states have only one imaginary frequency. Intrinsic reaction coordinate (IRC) calculations[28,29] are also performed so that a transition state connects two appropriate local minima in the reaction paths. The hybrid B3LYP exchange−correlation functional[30] is adopted. A contracted Gaussian basis set of triple zeta valence quality[31] plus one p function for H and V atoms and one d function for C and O atoms is used. This basis set is denoted as TZVP in Gaussian 03 program. This functional and basis set are tested to predict reasonably good energetics for vanadium oxides and hydrocarbons at moderate computational costs in several theoretical investigations.[7,8] Test calculations indicate that basis set superposition error (BSSE)[32,33] is negligible, so the BSSE is not taken into consideration in this study. The zero-point vibration corrected energies (ΔH_{0K}) and the Gibbs free energies at 298 K (ΔG_{298K}) are reported in this study. Cartesian coordinates, electronic energies, and vibrational frequencies for all of the optimized structures are available upon request.

3. Results

3.1. Reaction of VO_3 with C_3H_6. The following reaction channels are followed for the reaction of VO_3 with C_3H_6.

$$VO_3 + C_3H_6 \rightarrow VO_2CHCH_3 + HCHO \text{ (formaldehyde)} \qquad \Delta H_{298K} = -0.29 \text{ eV} \quad (1)$$

$$VO_3 + C_3H_6 \rightarrow VO_2CH_2 + CH_3CHO \text{ (acetaldehyde)} \qquad \Delta H_{298K} = -0.53 \text{ eV} \quad (2)$$

$$VO_3 + C_3H_6 \rightarrow VO_2 + CH_3CH_2CHO \text{ (propaldehyde)} \qquad \Delta H_{298K} = -0.65 \text{ eV} \quad (3)$$

$$VO_3 + C_3H_6 \rightarrow VO_2 + (CH_3)_2CO \text{ (acetone)} \qquad \Delta H_{298K} = -0.99 \text{ eV} \quad (4)$$

$$VO_3 + C_3H_6 \rightarrow VO_2 + C_3H_6O \text{ (propylene oxide)} \qquad \Delta H_{298K} = +0.39 \text{ eV} \quad (5)$$

$$VO_3 + C_3H_6 \rightarrow VO_2H_2 + CH_2{=}CHCHO \text{ (acrolein)} \qquad \Delta H_{298K} = -1.67 \text{ eV} \quad (6)$$

$$VO_3 + C_3H_6 \rightarrow VO_2C_3H_4 + H_2O \text{ (water)} \qquad \Delta H_{298K} = -1.00 \text{ eV} \quad (7)$$

The DFT calculated enthalpy of reaction at 298 K (ΔH_{298K}) is listed after each reaction. The potential energy profiles for reactions 1–7 are plotted in Figure 1. The structures and energies of the reaction intermediates and transition states are given in Figure 2. The vanadium species VO_3, VO_2, VO_2CH_2, $VO_2CH{-}CH_3$, and $VO_2C_3H_4$ have doublet ground states (Figure S1). For simplicity, crossing of spin doublet and quartet potential energy surfaces (spin conversion[35]) is not considered for reactions 1–5 and 7. The product VO_2H_2 has a quartet ground state, and its lowest doublet state is higher in energy by 1.41 eV (defined by ΔH_{0K}). Spin conversion is thus possible in later stages of reaction 6. As shown in Figure 1, doublet-quartet conversion is not required because formation of doublet VO_2H_2 is also thermodynamically favorable.

The formation of various partial oxidation products (HCHO, CH_3CHO, CH_3CH_2CHO, $(CH_3)_2CO$, and $CH_2{=}CHCHO$) in the reaction $VO_3 + C_3H_6$ is thermodynamically favorable. The formation of HCHO and CH_3CHO involves C=C bond cleavage, whereas formation of other products involves hydrogen transfers. Reactions 1–4 and 6 and 7 indicate that less heat of reaction (0.29 and 0.53 eV versus 0.65, 0.99, 1.00, and 1.67 eV) is released in the formation of the C=C bond cleavage products than in the formation of hydrogen transfer products, including $VO_2C_3H_4 + H_2O$. Figure 1a indicates that all of the thermodynamically allowed reactions are also kinetically favorable at 0 K; however, considering an equilibrium reaction at $T = 298$ K, Figure 1b indicates that all of the hydrogen transfer processes are subject to some overall free energy barriers: $\Delta G_{298K} = +0.01$ eV (Figure 2, Group 6, **4/12**, formation of H_2O and $CH_2{=}CHCHO$), +0.06 eV (Group 3, **8/9**, CH_3CH_2CHO), and +0.19 eV [Group 4, **3/10**, $(CH_3)_2CO$]. This is due to the entropy loss ($\Delta S < 0$) in the formation of reaction intermediates from the separated reactants VO_3 and C_3H_6. The entropy contribution ($-\Delta ST > 0$) puts the relative free energy

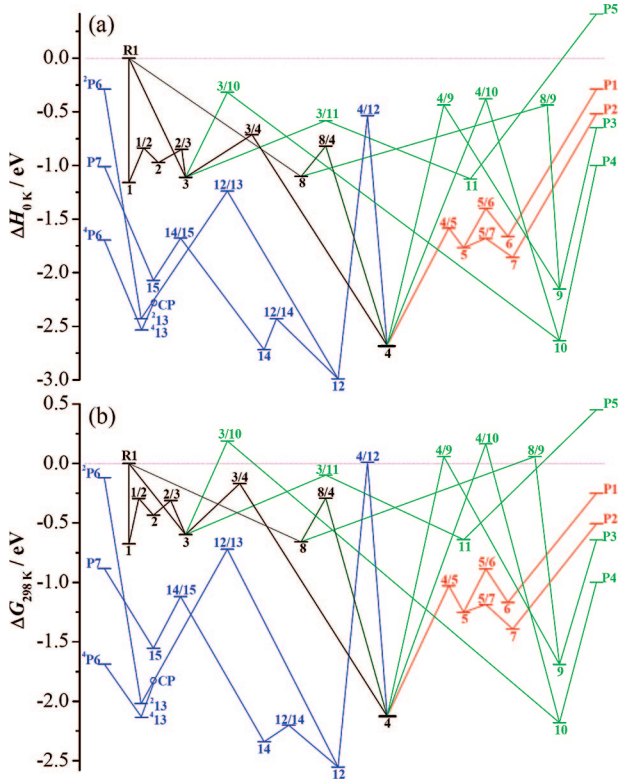

Figure 1. Potential energy profiles for the reaction of VO_3 with propylene. The profiles are plotted for zero-point vibration corrected energies (a) and Gibbs free energies at 298 K (b) relative to the separated reactants $VO_3 + C_3H_6$. The reaction intermediates and transition states are denoted as n and n_1/n_2, respectively. In the figure, **R1** = $VO_3 + C_3H_6$, **P1** = $VO_2CHCH_3 + HCHO$, **P2** = $VO_2CH_2 + CH_3CHO$, **P3** = $VO_2 + CH_3CH_2CHO$, **P4** = $VO_2 + (CH_3)_2CO$, **P5** = $VO_2 + C_3H_6O$, **P6** = $VO_2H_2 + CH_2{=}CHCHO$, and **P7**= $VO_2C_3H_4 + H_2O$. Superscripts 2 and 4 denote species in doublet and quartet spin states, respectively. "CP" denotes a possible spin conversion points for reaction **R1** → **P6** (see text for details).

above the relative enthalpy by about 0.5 eV for the reaction intermediates, whereas the relative energy positions of the separated products (P1−P7) do not change significantly. Because of relatively low barriers, the overall free energy barriers in the C=C bond cleavage process are still negative ($\Delta G_{298K} = -0.29$ eV, see Figure 2/Group 3 for **8/4**).

The critical reaction intermediate in the C=C bond cleavage process has a five-membered ring structure (**4** in Figure 2/Group 1) that is formed through a [3+2] cycloaddition. The cycloaddition processes ($VO_3 + C_3H_6$ → **1** → **1/2** → **2** → **2/3** → **3** → **3/4** → **4** or $VO_3 + C_3H_6$ → **8** → **8/4** → **4**) are overall barrierless. Formation of **4** results in a net energy release of 2.68 eV (ΔH_{0K}). The C=C bond in the C_3H_6 moiety becomes a single bond that is reflected by the lengthening of the C1−C2 bond length (0.155 nm in **4** vs 0.133 nm in free C_3H_6). The amount of energy released is sufficient to overcome the barrier (1.09 eV) in the C=C bond cleavage process (**4** → **4/5** → **5**). HCHO and CH_3CHO moieties are almost formed in **5** after this process. Two parallel processes **5** → **5/6** → **6** → **P1** and **5** → **5/7** → **7** → **P2** with no overall barriers cause formation of formaldehyde and acetaldehyde, respectively.

Starting from the cycloaddition intermediate **4**, a hydrogen transfer from the methyl group to a ring oxygen atom (O2) results in intermediate **12** (**4** → **4/12** → **12**). This process is subject to a high-energy barrier (2.14 eV) because **4** with the ring structure is energetically quite stable; however, the high energy (2.68 eV) released in the formation of **4** is sufficient to overcome this barrier. Considering entropy contribution ($-\Delta ST$), this hydrogen process is subject to a tiny positive (0.01 eV, Figure 2) overall free energy barrier at room temperature. Because **12** is even lower in energy than **4**, the subsequent processes that mainly involve transfer of a second hydrogen atom are overall barrierless. Acrolein (**P6**) and water (**P7**) can be formed starting from **12**: **12** → **12/13** → **13** → **P6**; **12** → **12/14** → **14** → **14/15** → **15** → **P7**.

Other critical reaction intermediates in the reaction of VO_3 with C_3H_6 are **3** and **8** (see Figures 1 and 2) that are formed through bonding between C1 or C2 with the single bonded oxygen atom (O3) in VO_3. Transfer of one hydrogen atom starting from these intermediates results in formation of propaldehyde (**8** → **8/9** → **9** → **P3**) and acetone (**3** → **3/10** → **10** → **P4**). Open structures **3** and **8** are not as stable as the ring structure **4**. Hydrogen transfers starting from open structures **3** and **8** are thus subject to lower barriers than they are starting from ring structure **4** (0.79 and 0.66 eV vs 2.30 and 2.22 eV, defined by ΔH_{0K}). As a result, net overall hydrogen transfer barriers are determined by a balance between energy release and consumption. The overall barriers to the formation of propaldehyde (**P3**) and acetone (**P4**) are similar (compare **4/9** with **8/9** and **4/10** with **3/10**).

Propylene oxide can be formed overall barrierlessly starting from intermediate **3** (**3** → **3/11** → **11**); however, a high binding energy (1.53 eV, see Figure 2) between propylene oxide and VO_2 prevents formation of separated products (VO_2 + propylene oxide) under room temperature conditions.

3.2. Reactions of VO_2CH_2, VO_2CHCH_3, and VO_3C with O_2. The following reaction channels are explored for the reaction of O_2 with VO_2CH_2 and $VO_2C_2H_4$ produced in reactions 2 and 1, respectively:

$$VO_2CH_2 + O_2 \rightarrow VO_3 + HCHO \qquad \Delta H_{298K} = -2.36 \text{ eV} \quad (8)$$

$$VO_2CHCH_3 + O_2 \rightarrow VO_3 + CH_3CHO \qquad \Delta H_{298K} = -2.60 \text{ eV} \quad (9)$$

$$VO_2CH_2 + O_2 \rightarrow VO_3C + H_2O \qquad \Delta H_{298K} = -3.31 \text{ eV} \quad (10)$$

$$VO_2CHCH_3 + O_2 \rightarrow VO_3C + CH_3OH \qquad \Delta H_{298K} = -2.65 \text{ eV} \quad (11)$$

The reaction pathway of O_2 with VO_3C, produced in reaction 10 or 11, is also followed:

$$VO_3C + O_2 \rightarrow VO_3 + CO_2 \qquad \Delta H_{298K} = -4.08 \text{ eV} \quad (12)$$

The potential energy profiles and intermediate structures for the reaction $VO_2CH_2 + O_2$ are plotted in Figures 3 and 4, respectively. Similar results are given in Figures S2 and S3 (Supporting Information) for $VO_2CHCH_3 + O_2$. Results for reaction of O_2 with VO_3C are given in Figure 5. The listed enthalpies of reaction indicate that reactions of O_2 with hydrocarbon and carbon containing vanadium oxide species (VO_2CH_2, VO_2CHCH_3, and VO_3C) are very exothermic. Barrierless reaction pathways are determined for all the reactions.

Figure 3 shows that formaldehyde + VO_3 and water + VO_3C can be formed with no overall barriers in the reaction of VO_2CH_2 with O_2. The O−O bond cleavage (**18** → **18/19** → **19** and **21** → **21/22** → **22**, see Figure 4) is a critical part of the reaction. Cleavage occurs after rearrangement of the

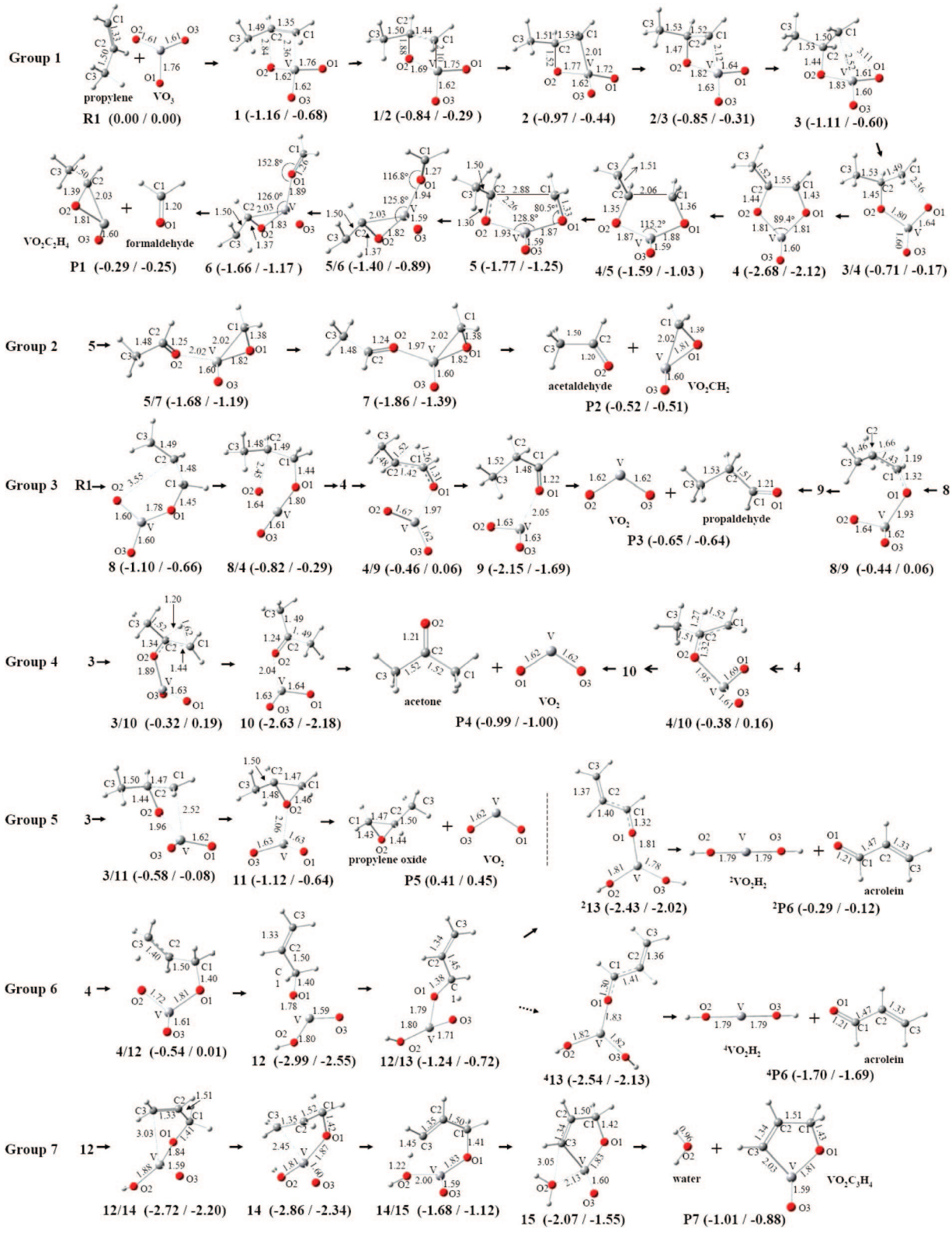

Figure 2. Optimized structures and energies of the species in Figure 1. The energies (in eV) are given as ($\Delta H_{0K}/\Delta G_{298K}$) below each geometry. The bond lengths in 0.1 nm and some bond angles in degrees are given. The structures are grouped according to reactions 1–7 in the text.

O_2 moiety over VO_2CH_2 that forms appropriate peroxo-species **18** and **21**. After O−O bond cleavage, the large amount of heat of formation (3.75 and 3.35 eV) can be used to evaporate the formaldehyde molecule (**19** → VO_3 + HCHO) or to rearrange the reaction complex further to cause water formation (**22** → **22/23** → **23** → **23/25** → **25** → **25/26** → **26** → **26/27** → **27** → $VO_3C + H_2O$). Figures S2 and S3 show similar reaction processes for the reaction $VO_2CHCH_3 + O_2$; this reaction can be considered as the same as the previous one, except that one of the hydrogen atoms of VO_2CH_2 is changed to a methyl group. Acetaldehyde + VO_3 and methanol + VO_3C can also be formed overall barrierlessly in the reaction. For methanol formation, the methyl group cannot transfer as a hydrogen atom does. As a result,

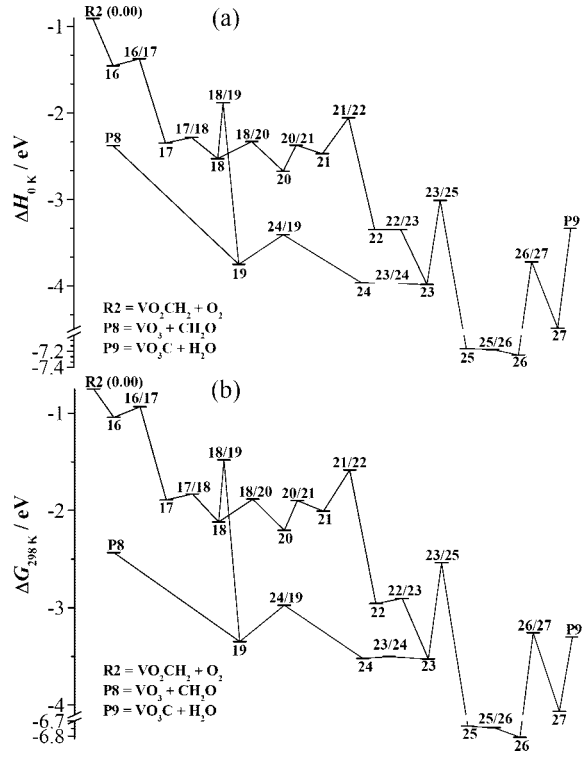

Figure 3. Potential energy profiles for the reaction of VO_2CH_2 with O_2. The profiles are plotted for zero-point vibration corrected energies (a) and Gibbs free energies at 298 K (b) relative to the separated reactants $VO_2CH_2 + O_2$. The reaction intermediates and transition states are denoted as n and n_1/n_2, respectively.

the hydrogen transfers in $VO_2CHCH_3 + O_2$ and those in $VO_2CH_2 + O_2$ are not similar. The details can be seen by comparing Figure 4 with S3 for the last group of the structures connected by arrows.

Figure 5 shows that the model catalyst VO_3 can also be regenerated overall barrierlessly by reaction of a second O_2 molecule with carbonized vanadium oxide species VO_3C produced in reactions 10 and 11. Similar to reactions 8–11, O−O bond cleavage can be considered as a critical part of the reaction.

4. Discussion

4.1. Comparison of the DFT Results with Gas Phase Experimental Observations. An experimental study employing single photon ionization through radiation generated by a soft X-ray laser and mass detection through a time of flight (TOF) spectrometer has been recently carried out on the reaction of neutral vanadium oxide clusters with propylene in the gas phase, under near room temperature conditions. Figure 6 plots the TOF mass spectrum in the mass range of 60−160 amu for the reactions of neutral V_mO_n clusters with C_3H_6. The experimental conditions are similar to those used for $V_mO_n + C_2H_4$ in ref 14 and complete results, including those with several other unsaturated hydrocarbons, will be presented in a separate paper.[34] The reaction products VO_2CH_2, $VO_2C_2H_4$, $VO_2C_3H_4$, and possibly VO_2H_2 (the signal of which is overlapped with the shoulder of the unreacted VO_2 feature) are observed. The current DFT study (Figures 1 and 2) suggests that the observed VO_2CH_2 and $VO_2C_2H_4$ products are formed from $VO_3 + C_3H_6$, as reactions 1 and 2 have negative overall free energy barriers at room temperature. Figures 1a and 2 show that the ΔH_{0K} value of **4/12** (critical transition state leading to $VO_2C_3H_4$ formation) is −0.54 eV, which is lower than those of P1 ($VO_2C_2H_4 + HCHO$, −0.29 eV) and P2 ($VO_2CH_2 + CH_3CHO$, −0.52 eV). These results indicate that the experimentally observed $VO_2C_3H_4$ is also generated from the reaction $VO_3 + C_3H_6$, given that the reaction intermediates are not fully at thermal equilibrium due to the relatively low pressure (∼1 Torr) of the gas phase flow cell experiments.[14,34] The formation of $VO_2 + CH_3CH_2CHO$ and $VO_2 + (CH_3)_2CO$ is also possible considering the negative ΔH_{0K} values for the critical transition states (**8/9** and **3/10**) for the reactions 3 and 4; however, one cannot easily differentiate the product VO_2 from the unreacted VO_2 in the neutral cluster reactivity study.

In Figure 1, **4** is a common intermediate involved in the formation of P1−P4, P6, and P7. On the basis of the Rice−Ramsberger−Kassel−Markus (RRKM) theory, one can expect that product formation with lower barriers will (with some allowance for dynamical considerations) always dominate. The ΔH_{0K} values (see Figures 1a and 2) of the critical barriers are −0.54 eV (**4/12**), −0.52 eV (**P2**), −0.46 eV (**4/9**), −0.38 eV (**4/10**), and −0.29 eV (**P1**). As a result, $VO_2C_3H_4$ ($+H_2O$) and VO_2CH_2 ($+CH_3CHO$) will be the dominant products coming from intermediate **4** in the experiment. Figure 6 does show that the mass signals of $VO_2C_3H_4$ and VO_2CH_2 are relatively strong with respect to that of $VO_2C_2H_4$. The ΔH_{0K} value of **P1** (−0.29 eV) is the highest among the five listed barriers. Given that the ionization efficiencies of the vanadium species are similar, observation of comparable mass signals for $VO_2C_2H_4$, $VO_2C_3H_4$, and VO_2CH_2 implies that the entropy [**4 → 4/5 → 5 → 5/6 → P1**] is more favorable than that for [**4 → 4/12 → 12**] (see Figure 1b), and other dynamical issues, such as state locations and densities of a specific vibration, may influence formation of $VO_2C_2H_4$. Although the current DFT study cannot provide an accurate quantitative prediction for the product abundances in the $VO_3 + C_3H_6$ reaction, the calculated predictions are in qualitative agreement with the experimental observations for VO_2CH_2, $VO_2C_2H_4$, and $VO_2C_3H_4$.

4.2. Complexity of the Reactions. The DFT results reported in this study represent reaction channels with negative or small positive overall free energy barriers. The choice of reaction channels is guided by formation of stable products with low reaction barriers. We have not attempted to determine all the possible reaction intermediates and channels, which is hard to achieve for a 13 atom reaction system such as $VO_3 + C_3H_6$. Figure 7 gives an example of the challenge involved in investigating all the possible reaction channels in the sub-reaction $VO_3 + C_3H_6 \rightarrow VO_2C_2H_4 + HCHO$. Four isomers are determined for $VO_2C_2H_4$ ((a)−(d) in Figure 7). VO_2CHCH_3 in reaction 1 has highest energy among the four isomers. In following the reaction pathway, a good deal of effort has been devoted to finding allowed pathways to produce $VO_2C_2H_4$ isomers other than VO_2CHCH_3. This involves transfer of a hydrogen atom from the methyl group starting from an appropriate reaction intermediate. Two attempts (TS1 and TS2 in Figure 6) are made for this transfer and the two hydrogen transfers are subject to overall barriers 0.81 and 0.23 eV (defined by ΔH_{0K}) that are significantly higher than the energy of the separated reactants ($VO_3 + C_3H_6$).

4.3. Comparison of $VO_3 + C_3H_6$ with $VO_3 + C_2H_4$ and Other Related Reactions. In a previous DFT study,[14] we showed that the reaction of $VO_3 + C_2H_4$ produces $VO_2CH_2 +$ HCHO barrierlessly. The results are supported by experimental observations: disappearance of reactants VO_3 accompanied by the appearance of product species VO_2CH_2 in the reaction of neutral vanadium oxide clusters with C_2H_4. The HCHO and CH_3CHO product formation in the reaction of $VO_3 + C_3H_6$ is thus expected. This has been verified in the present study. The

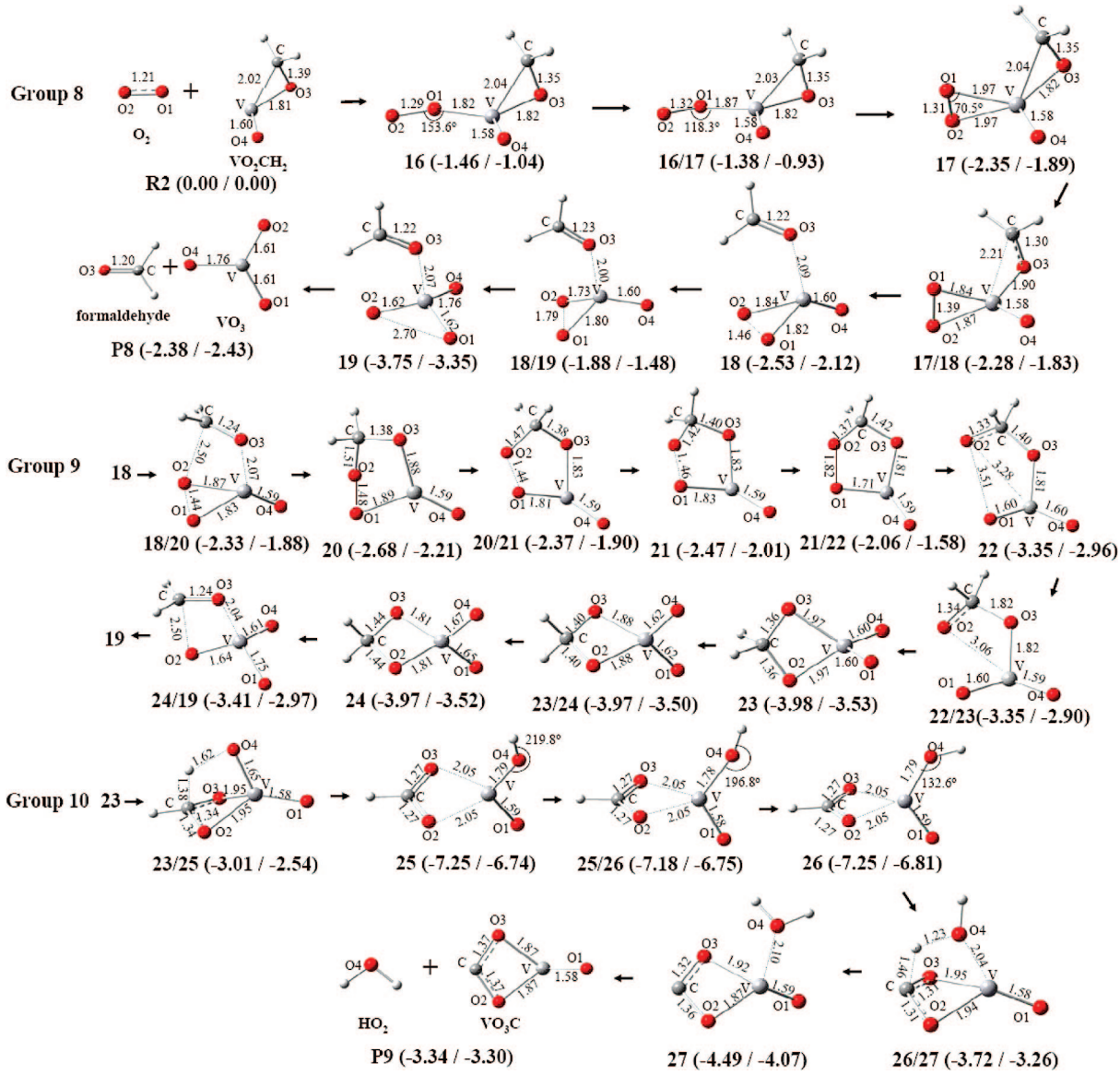

Figure 4. Optimized structures and energies of the species in Figure 3. The energies (in eV) are given as ($\Delta H_{0K}/\Delta G_{298K}$) below each geometry. The bond lengths in 0.1 nm and some bond angles in degrees are given.

generality of the cleavage of C═C bonds in the reaction of alkenes with VO_3 can be summarized as: the large amount of energy released in the [3+2] cycloaddition process is sufficient to break the weakened C═C bond (such as C1−C2 of **4** in Figure 2) and evaporate an aldehyde fragment. In addition to the above similarity between the reactions of $VO_3 + C_3H_6$ and $VO_3 + C_2H_4$, the added methyl group in C_3H_6 results in reaction channels 7 and possibly 6. Such a mechanism is supported by experiment, as shown in Figure 6. As in the C═C bond cleavage process, reaction channels 6 and 7 take advantage of the large heat of reaction in the [3+2] cycloaddition to overcome the reaction barrier for hydrogen transfer from the methyl group to one oxygen atom (**4** → **4/12** → **12** in Figure 1). A detailed comparison shows that direct C_x aldehyde formation ($VO_3 + C_xH_{2x} \rightarrow VO_2 + C_xH_{2x}O$) is subject to lower free energy barriers for $x = 3$ than for $x = 2$ (0.06 eV vs 0.18 eV).

Harvey et al. investigated the reaction of $VO_2^+ + C_2H_4$ nearly ten years ago by both experiment and theory.[5] Gracia et al. recently studied the same reaction,[11] as well as the reaction $VO_2^+ + C_3H_6$,[12] by DFT calculations. By a spin conversion mechanism,[5,11,35] acetaldehyde can be formed overall barrierlessly in $VO_2^+ + C_2H_4$, in agreement with the experimental results.[5] The reaction of VO_2^+ with C_3H_6 is predicted to form acetone, propaldehyde, allene, and propyne as thermodynamically and kinetically allowed products. Reactions of $V_2O_5^+$ and $V_4O_{10}^+$ with C_2H_4 have also been investigated by DFT calculations.[7,9] Formation of acetaldehyde in both reactions is highly favorable and supports the experimental observations of $V_2O_4^+$ and $V_4O_9^+$ as reaction products.[7] Because the [3(OVO)+2 (C═C)] cycloaddition structure may not be stable in the $VO_2^+ +$ alkene reactions, no reaction involving C═C bond cleavage is discussed. In the reaction $V_2O_5^+ + C_2H_4$, a [3+2] cycloaddition species is predicted to be lower in energy than the separated reactants by 4.44 eV. As can be seen from the results in Figures 1 and 2, this high energy should be able to cleave the C═C bond and evaporate formaldehyde fragment(s). The authors did suggest a side reaction channel, $V_2O_5^+ + C_2H_4 \rightarrow V_2O_3^+ + 2HCHO$ ($\Delta E = -0.65$ eV),[9] to explain observation of $V_2O_3^+$ as minor product in the experiments.

In addition to the C═C bond cleavage reactions, exothermic processes are predicted for direct oxygenation reactions $VO_3 + C_xH_{2x} \rightarrow VO_2 + C_xH_{2x}O$ and $VO_2^+/V_2O_5^+/V_4O_{10}^+ + C_xH_{2x} \rightarrow VO^+/V_2O_4^+/V_4O_9^+ + C_xH_{2x}O$, in which $C_xH_{2x}O$ is acetaldehyde ($x = 2$), propaldehyde ($x = 3$), or acetone ($x = 3$). These

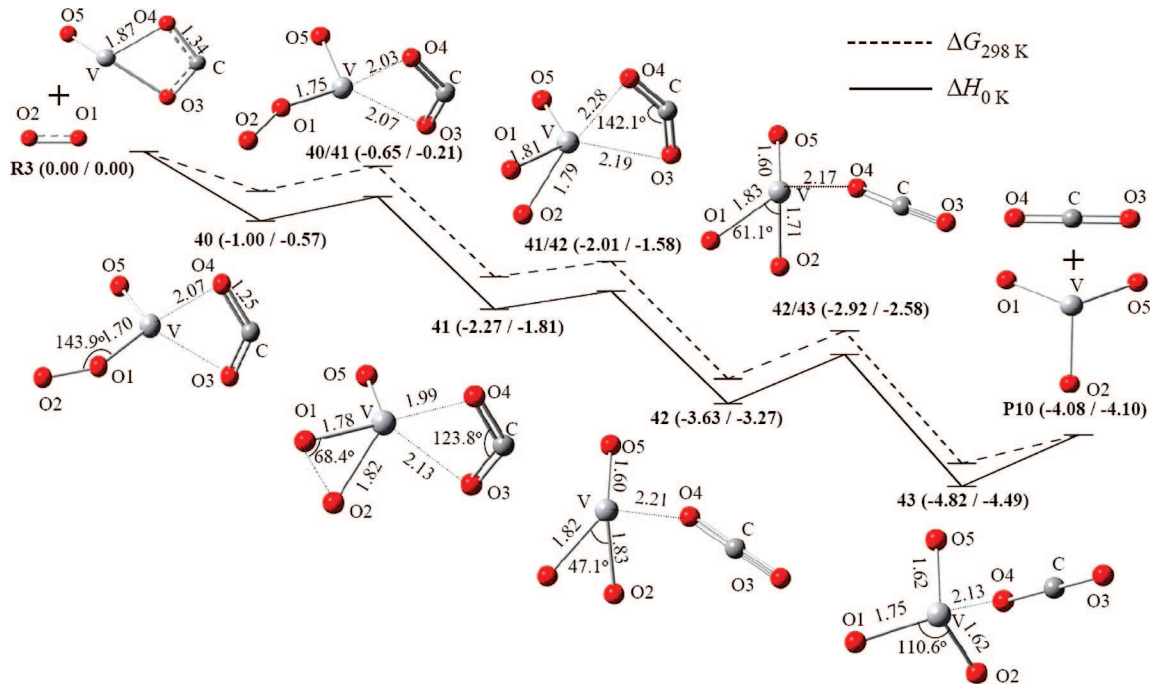

Figure 5. Potential energy profiles and optimized structures of reaction intermediates (n) and transition states (n_1/n_2) for $VO_3C + O_2$. The zero-point vibration corrected energy (ΔH_{0K}) profile is below the Gibbs free energy (ΔG_{298K}) profile. The energies (in eV) are given as ($\Delta H_{0K}/\Delta G_{298K}$) for each structure. The bond lengths in 0.1 nm and some bond angles in degrees are given.

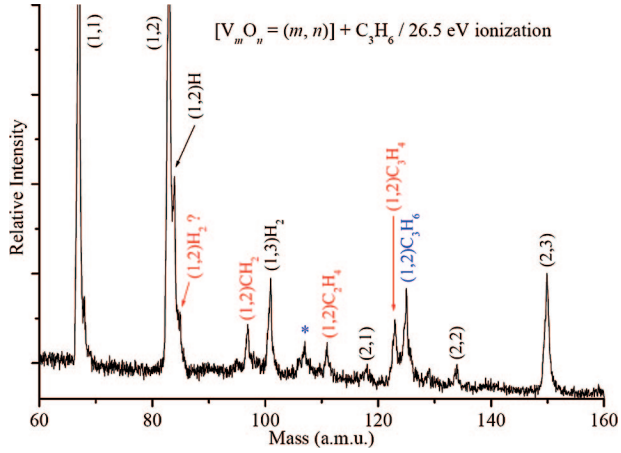

Figure 6. TOF mass spectrum in the mass range of 60−160 amu for the reactions of neutral V_mO_n clusters with C_3H_6. The symbol (m, n) denotes V_mO_n. The four carbon containing clusters VO_2CH_2, $VO_2C_2H_4$, $VO_2C_3H_4$, and $VO_2C_3H_6$ are new species (products) after the reactions/collisions with C_3H_6. An asterisk marks a peak with mass of 107 amu that can be assigned as VOC_3H_4 ($VO_2 + C_3H_6 \rightarrow VOC_3H_4 + H_2O$?).

reaction processes can be divided into three phases: (1) formation of species with structure $V-O-C_xH_{2x}$, in which the O atom is single-bonded with the C1 (or C2) atom or bridge-bonded with both C1 and C2 atoms; (2) transfer of a hydrogen atom from an O bonded C atom to form species $V\cdots O{=}C_xH_{2x}$, in which the O atom is nearly double-bonded with one carbon atom; (3) evaporation of an $O{=}C_xH_{2x}$ fragment from the vanadium oxide cluster. Phases 1 and 3 proceed with no overall free energy barrier in all of the DFT studied reactions. Phase 2 in the reactions involving the cationic species ($VO_2^+/V_2O_5^+/V_4O_{10}^+ + C_xH_{2x}$) also proceeds with no overall barriers. In contrast, phase 2 of neutral species reactions ($VO_3 + C_xH_{2x}$) is subject to overall free energy barriers (0.06−0.19 eV) according to the DFT calculations. Another major difference between neutral and cationic reaction systems is that in phase 3 more free energy (1.99−2.66 eV versus 1.05−1.18 eV, defined by ΔG_{298K}) is needed to evaporate $O{=}C_xH_{2x}$ from the cationic $VO^+/V_2O_4^+/V_4O_9^+$ structure than from neutral VO_2.

4.4. Gas Phase Catalytic Cycles. Figure 8 summarizes the barrierless reaction channels that form catalytic cycles for C_3H_6 partial oxidation by O_2 facilitated by the model catalyst VO_3 under gas phase, room temperature conditions. In Figures 1 and 2, **5/6** and **P1** ($VO_2CHCH_3 + HCHO$) are higher in energy than **5/7** and **P2** ($VO_2CH_2 + CH_3CHO$), respectively, so the formation of CH_3CHO is more favorable than that of HCHO for the $VO_3 + C_3H_6$ reaction. In the reaction $VO_2CH_2 + O_2$ (Figures 3 and 4), the product $VO_3C + H_2O$ is thermodynamically and kinetically more favorable than the product $VO_3 +$ HCHO. We thus conclude that CH_3CHO (with H_2O and CO_2) will be selectively more abundant among the partial oxidation products (CH_3CHO, HCHO, and CH_3OH) in the reaction of $C_3H_6 + O_2$ catalyzed by VO_3 at room temperature.

The current DFT calculations predict that the C═C bond cleavage products VO_2CHCH_3 and VO_2CH_2 are readily oxidized by O_2 at room temperature to reproduce the VO_3. In the gas phase experimental study of neutral vanadium oxide clusters reacting with C_2H_4 and C_3H_6, HCHO/CH_3CHO are derived as part of the bond cleavage products in reactions such as $VO_3 + C_3H_6 \rightarrow VO_2CH_2 + CH_3CHO$; however, these aldehydes are not observed probably due to their low concentrations. These products could perhaps be observed by taking advantage of the catalytic cycles in Figure 8, because the concentration of products such as CH_3CHO will be increased if a mixed gas of O_2 and C_3H_6, rather than pure C_3H_6, were used as the reactant.

4.5. Consideration of Condensed Phase Catalysis. Molecular level reaction mechanisms in complex condensed phase heterogeneous catalysis are difficult to establish by model catalytic studies using a single vanadium cluster; nonetheless, various reaction channels in this study do parallel similar behavior in propylene selective oxidation over various vanadium oxide catalysts.[16–19] The current study indicates that the formation of various useful product aldehydes (propaldehyde, acetal-

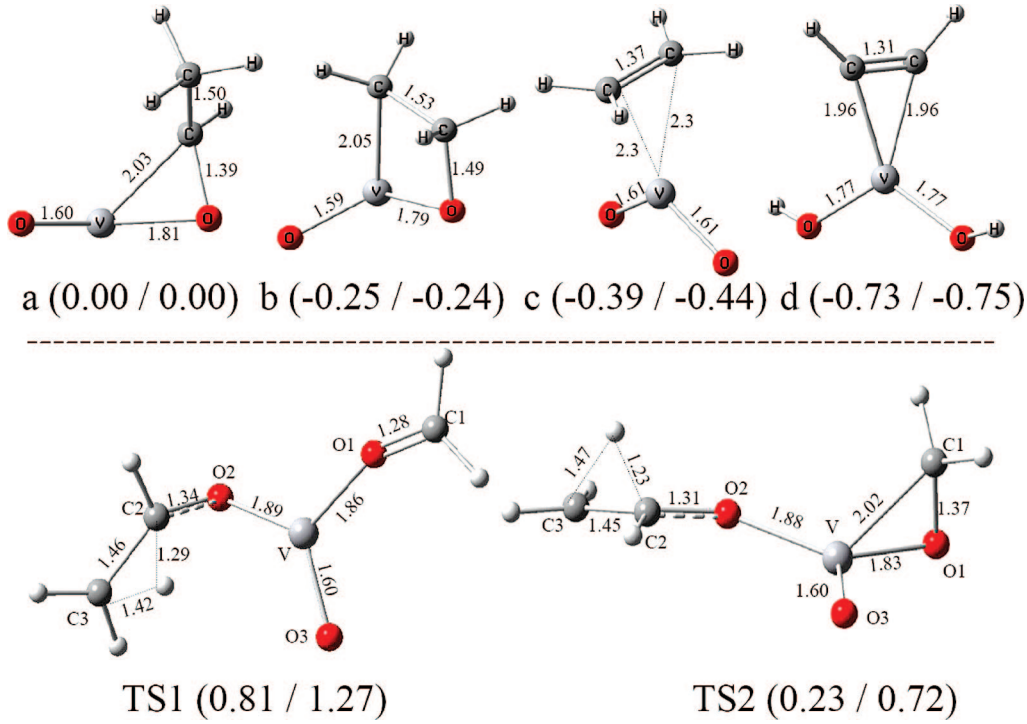

Figure 7. Optimized structures and energies of four isomers (a)−(d) of $VO_2C_2H_4$ (upper panel); optimized structures and energies of two transition states (TS1 and TS2) in reaction $VO_3 + C_3H_6$ to form the CH_2CH_2 moiety (lower panel). The energies (in eV) relative to VO_2CHCH_3 (for isomers (a)−(d)) or relative to reactants $VO_3 + C_3H_6$ (for TS1 and TS2) are given as ($\Delta H_{0K}/\Delta G_{298K}$) below each geometry. The bond lengths in 0.1 nm are given.

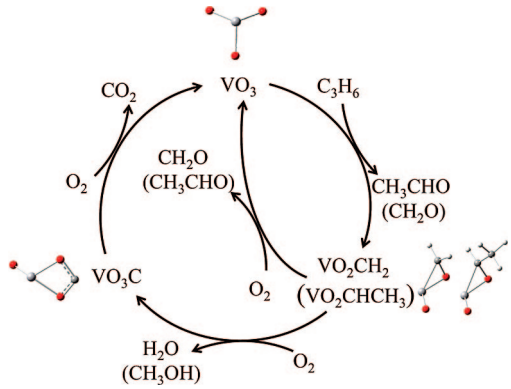

Figure 8. Schematic diagram showing barrierless reaction channels that form catalytic cycles for propylene (C_3H_6) partial oxidation over the VO_3 cluster under gas phase, room temperature conditions.

dehyde, formaldehyde), acrolein, and acetone can be generated with negative or small positive overall barriers in the reaction of VO_3 with propylene. Moreover, VO_3 can be regenerated easily in selected reactions. In the selective oxidation of propylene over vanadium oxide catalysts, highly selective formation of acetaldehyde,[18,19] acrolein,[17] and acetone[16] are observed depending on the specific catalysts used. The DFT study in this work gives molecular level insight in to how these products may be formed. It is interesting to note that acetaldehyde and carbon dioxide are the major products in propylene selective oxidation over V_2O_5/SiO_2.[18] The DFT calculations predict that formation of these two products is also the most favorable in model catalytic cycles (Figure 8). To explain formation of acetaldehyde from propylene oxidation in heterogeneous catalysis, Ruszel et al., suggest that electrophilic surface oxygen species O_2^- or O^- add to a C═C double bond with formation of peroxo or oxo intermediates that can decompose with breaking of a C−C bond.[18] The mechanism of surface O_2^- species adding to the C═C double bond is similar to the [3+2] cycloaddition found for the reaction of VO_3 with C_3H_6.

The above mentioned comparison between condensed phase and gas phase investigations raises the following interesting question: how realistic is the VO_3 cluster for modeling condensed phase vanadium oxide chemistry? In cluster chemistry, both open-shell (e.g., $V_2O_5^+$ and $V_4O_{10}^+$,[7,8b] and VO_3 in this study) and closed-shell (e.g., VO_2^+ and $V_3O_7^+$)[5,8a] clusters are used as prototypes for identification of active centers of bulk or supported vanadium oxides. Different clusters usually possess different reactivities and the open-shell clusters are typically more reactive.[5] From the point view of thermodynamics, one does not expect that a stable oxide surface is covered with active centers that can be fully modeled by open-shell radical clusters; however, the radical clusters may serve as (1) models of oxygen-rich or oxygen-poor surface defects and (2) intermediate reactive centers during catalytic processes. (Note that some surface oxygen species have extremely short lifetimes.[17]) In this study, although the oxygen-rich cluster VO_3 is very oxidative and thus unstable in a reducing environment, it can be recycled (Figure 8) through the reaction of O_2 with the oxygen-poor intermediates (VO_2CH_2, VO_2CHCH_3, and VO_3C with the vanadium being in +4 oxidation state). As mentioned above, the C_3H_6 partial oxidation products over specific condensed phase vanadium oxides (V_2O_5/SiO_2)[18] and over the VO_3 cluster are similar. Thus, we suggest the use of surface characterization techniques to identify some possible new surface species in the selective oxidation of C_3H_6 over vanadium oxide catalysts. A candidate for this species is the one with a five-membered ring structure (similar to **4** in Figure 2) that can be formed with no overall barrier and is energetically quite stable. The vanadium is in a +4 oxidation state in this ring structure.

5. Conclusions

The reaction of neutral VO_3 with propylene produces acetaldehyde ($VO_2CH_2 + CH_3CHO$) or formaldehyde ($VO_2CHCH_3 + HCHO$) overall barrierlessly under room temperature conditions. With previous findings of formaldehyde formation ($VO_2CH_2 + HCHO$) in the reaction of VO_3 with ethylene, a general mechanism of C═C bond cleavage of alkenes over VO_3 may be concluded: the heat of reaction in the barrierless [3+2] cycloaddition is sufficient to break the C═C bond and to evaporate an aldehyde fragment. The hydrogen transfer barrier from the methyl group to one oxygen atom can be overcome by using the heat of reaction in the [3+2] cycloaddition, which finally leads to formation of water ($VO_2C_3H_4 + H_2O$) or acrolein ($VO_2H_2 + CH_2$═$CHCHO$) in the reaction $VO_3 + C_3H_6$. Formation of acetone and propaldehyde is subject to small overall free energy barriers for the reaction $VO_3 + C_3H_6$. Gas phase catalytic cycles are provided by studying reactions of O_2 with C═C bond cleavage products (VO_2CH_2 and VO_2CHCH_3). These reactions are facile under room temperature conditions and can recycle the VO_3. The DFT predictions of several reaction channels (formation of CH_3CHO, HCHO, and H_2O in the $VO_3 + C_3H_6$ reaction) have been supported by recent gas phase experimental observations. Other DFT results, such as the gas phase catalytic cycles and involvement of the [3+2] cycloaddition intermediates in related reactions, may be verified by further experiments.

Acknowledgment. This work was supported by the Chinese Academy of Sciences (Hundred Talents Fund), the National Natural Science Foundation of China (No. 20703048), the 973 Programs (Nos. 2006CB932100 and 2006CB806200), the NSF ERC for EUV S&T, the USDOE, the USAFOSR, and PM USA.

Supporting Information Available: Optimized structures and relative free energies of VO_3, VO_2CH_2, VO_2CHCH_3, and $VO_2C_3H_4$ in the doublet and quartet spin multiplicities (Figure S1). Potential energy profiles for the reaction $VO_2CHCH_3 + O_2$ (Figure S2). Optimized structures and relative energies of the species in the reaction channel of $VO_2CHCH_3 + O_2$ (Figure S3). This material is available free of charge via the Internet at http://pubs.acs.org.

References and Notes

(1) Ertl, G.; Knozinger, H. and Weikamp, J. *Handbook of Heterogeneous Catalysis*; Wiley-VCH: New York, 1997.

(2) Weckhuysen, B. M.; Keller, D. E. *Catal. Today* **2003**, *78*, 25.

(3) Fierro, J. L. G. *Metal Oxides*; Taylor & Francis Group, LLC: London, 2006.

(4) (a) Zemski, K. A.; Justes, D. R.; Castleman, A. W. *J. Phys. Chem. B* **2002**, *106*, 6136. (b) Foltin, M.; Stueber, G. J.; Bernstein, E. R. *J. Chem. Phys.* **1999**, *111*, 9577. (c) Fielicke, A.; Rademann, K. *Phys. Chem. Chem. Phys.* **2002**, *4*, 2621. (d) Schröder, D.; Engeser, M.; Bronstrup, M.; Daniel, C.; Spandl, J.; Hartl, H. *Int. J. Mass Spectrom.* **2003**, *228*, 743. (e) Schröder, D.; Loos, J.; Engeser, M.; Schwarz, H.; Jankowiak, H.C.; Berger, R.; Thissen, R.; Dutuit, O.; Dobler, J.; Sauer, J. *Inorg. Chem* **2004**, *43*, 1976. (f) Asmis, K. R.; Meijer, G.; Brümmer, M.; Kaposta, C.; Santambrogio, G.; L., W.; Sauer, J. *J. Chem. Phys* **2004**, *120*, 6461. (g) Molek, K. S.; Jaeger, T. D.; Duncan, M. A. *J. Chem. Phys.* **2005**, *123*, 144313. (h) Feyel, S.; Schröder, D.; Schwarz, H. *J. Phys. Chem. A* **2006**, *110*, 2647. (i) Feyel, S.; Scharfenberg, L.; Daniel, C.; Hartl, H.; Schröder, D.; Schwarz, H. *J. Phys. Chem. A* **2007**, *111*, 3278. (j) Fielicke, A.; Mitric, R.; Meijer, G.; Bonacic-Koutecky, V.; Helde, G. *J. Am. Chem. Soc.* **2003**, *125*, 15716. (k) Engeser, M.; Schlangen, M.; Schröder, D.; Schwarz, H.; Yumura, T.; Yoshizawa, K. *Organometallics* **2003**, *22*, 3933–3943. (l) Asmis, K. R.; Brümmer, M.; Kaposta, C.; Santambrogio, G.; Von Helden, G.; Meijer, G.; Rademann, K.; Wöste, L. *Phys. Chem. Chem. Phys.* **2002**, *4*, 1101. (m) Zhai, H. J.; Wang, L. S. *J. Chem. Phys.* **2002**, *117*, 7882. (n) Zhai, H. J.; Döbler, J.; Sauer, J.; Wang, L. S. *J. Am. Chem. Soc.* **2007**, *129*, 13270. (o) Waters, T.; Wedd, A. G.; O'Hair, R. A. J. *Chem. Eur. J.* **2007**, *13*, 8818. (p) Wang, W. -G.; Wang, Z. -C.; Yin, S.; He, S. -G.; Ge, M.-F. *Chin, J. Chem. Phys* **2007**, *20*, 4–412.

(5) Harvey, J. N.; Diefenbach, J. N.; Schröder, D.; Schwarz, H. *Int. J. Mass Spectrom.* **1999**, *182/183*, 85.

(6) Zemski, K. A.; Justes, D. R.; Castleman, A. W., Jr. *J. Phys. Chem. A* **2001**, *105*, 10237.

(7) Justes, D. R.; Mitric, R.; Moore, N. A.; Bonacic-Koutecky, V.; Castleman, A. W., Jr. *J. Am. Chem. Soc* **2003**, *125*, 6289.

(8) (a) Feyel, S.; Schröder, D.; Rozanska, X.; Sauer, J.; Schwarz, H. *Angew. Chem. Int. Ed.* **2006**, *45*, 4677. (b) Feyel, S.; Dobler, J.; Schröder, D.; Sauer, J.; Schwarz, H. *Angew. Chem. Int. Ed.* **2006**, *45*, 4681.

(9) Justes, D. R.; Castleman, A. W.; Mitric, R.; Bonacic-Koutecky, V. *Eur. Phys. J. D* **2003**, *24*, 331.

(10) (a) Vyboishchikov, S. F.; Sauer, J. *J. Phys. Chem. A* **2000**, *104*, 10913. (b) Vyboishchikov, S. F.; Sauer, J. *J. Phys. Chem. A* **2001**, *105*, 8588. (c) Calatayud, M.; Silvi, B.; Andres, J.; Beltran, A. *Chem. Phys. Lett.* **2001**, *333*, 493. (d) Calatayud, M.; Andres, J.; Beltran, A. *J. Phys. Chem. A* **2001**, *105*, 9760. (e) Calatayud, M.; Andres, J.; Beltran, A.; Silvi, B. *Theor. Chem. Acc.* **2001**, *105*, 299. (f) Calatayud, M.; Andres, J.; Beltran, A. *J. Phys. Chem. A* **2001**, *105*, 9760. (g) Calatayud, M.; Berski, S.; Beltran, A.; Andres, J. *Theor. Chem. Acc.* **2002**, *108*, 12. (h) Pykavy, M.; van Wullen, C. *J. Phys. Chem. A* **2003**, *107*, 5566. (i) Gracia, L.; Sambrano, J. R.; Safont, V. S.; Calatayud, M.; Beltran, A.; Andres, J. *J. Phys. Chem. A* **2003**, *107*, 3107. (j) Cheng, M. J.; Chenoweth, K.; Oxgaard, J.; Duin, A.; Goddard, W. A. *J. Phys. Chem. C* **2007**, *111*, 5115.

(11) Gracia, L.; Andres, J.; Safont, V. S.; Beltran, A. *Organometallics* **2004**, *23*, 730–739.

(12) Gracia, L.; Sambrano, J. R.; Andres, J.; Beltran, A. *Organometallics* **2006**, *25*, 1643–1653.

(13) (a) Matsuda, Y.; Bernstein, E. R. *J. Phys. Chem. A* **2005**, *109*, 314. (b) Matsuda, Y.; Bernstein, E. R. *J. Phys. Chem. A* **2005**, *109*, 3803. (c) Matsuda, Y.; Shin, D. N.; Bernstein, E. R. *J. Chem. Phys.* **2004**, *120*, 4142. (d) Shin, D. N.; Matsuda, Y.; Bernstein, E. R. *J. Chem. Phys.* **2004**, *120*, 4157. (e) Matsuda, Y.; Shin, D. N.; Bernstein, E. R. *J. Chem. Phys.* **2004**, *120*, 4165. (f) Dong, F.; Heinbuch, S.; He, S.-G.; Xie, Y.; Rocca, J. J.; Bernstein, E. R. *J. Chem. Phys.* **2006**, *125*, 164318. (g) He, S.-G.; Xie, Y.; Guo, Y.; Bernstein, E. R. *J. Chem. Phys.* **2007**, *126*, 194315.

(14) Dong, F.; Heinbuch, S.; Xie, Y.; Rocca, J. J.; Bernstein, E. R.; Wang, Z. C.; Deng, K.; He, S. G. *J. Am. Chem. Soc* **2008**, *130*, 1932.

(15) (a) Xu, X.; Friend, C. M. *J. Am. Chem. Soc.* **1991**, *113*, 6779. (b) Stangland, E.E.; Stevens, K.B.; Andres, R. P. W.; Delgass, N. *J. Catal.* **2000**, *191*, 332. (c) Xie, J.; Zhang, Q.; Chuang, K. T. *J. Catal.* **2000**, *191*, 86. (d) Berkessel, A.; Brandenburg, M. *Org. Lett.* **2006**, *8*, 20–4401. (e) Amano, F.; Yamaguchi, T.; Tanaka, T. *J. Phys. Chem. B* **2006**, *110*, 281. (f) Su, Z.; Borho, N.; Xu, Y. *J. Am. Chem. Soc.* **2006**, *128*, 17127. (g) Moens, B.; Winne, H.D.; Corthals, S.; Poelman, H.; Gryse, R.D.; Meynen, V.; Cool, P.; Sels, B.F.; Jacobs, P.A. *J. Catal.* **2007**, *247*, 86.

(16) Li, M.; Shen, J. *J. Catal.* **2002**, *205*, 248.

(17) Zhao, C.; Wachs, I. E. *Catal. Today* **2006**, *118*, 332.

(18) Ruszel, M.; Grzybowska, B.; Gasior, M.; Samson, K.; Gressel, I.; Stoch, J. *Catal. Today* **2005**, *99*, 151.

(19) Seiyama, T.; Nita, K.; Maehara, T.; Yamazoe, N.; Takita, Y. *J. Catal.* **1997**, *49*, 164.

(20) (a) Deo, G.; Wachs, I. E.; Haber, J. *Crit. Rev. Surf. Chem.* **1994**, *4*, 141. (b) Weckhuysen, B. M.; Wachs, I. E. In *Handbook of Surface and Interfaces of Materials Vol.1*; Nalwa, H. S., Ed.; Academic Press: San Diego, 2001; p 613. (c) Wachs, I. E.; Weckhuysen, B. M. *Appl. Catal. A: Gen.* **1997**, *157*, 67.

(21) (a) Gijzeman, O. L. J.; van Lingen, J. N. J.; van Lenthe, J. H.; Tinnemans, S. J.; Keller, D. E.; Weckhuysen, B. M. *Chem. Phys. Lett.* **2004**, *397*, 277. (b) Keller, D. E.; de Groot, F. M. F.; Koningsberger, D. C.; Weckhuysen, B. M. *J. Phys. Chem. B* **2005**, *109*, 10223. (c) Keller, D. E.; Koningsberger, D. C.; Weckhuysen, B. M. *J. Phys. Chem. B* **2006**, *110*, 14313. (d) Lingen, J. N. J.; Gijzeman, O. L. J.; Weckhuysen, B. M.; van Lenthe, J. H. *J. Catal.* **2006**, *239*, 34.

(22) Keller, D. E.; Visser, T.; Soulimani, F.; Koningsberger, D. C.; Weckhuysen, B. M. *Vibr. Spectrosc.* **2007**, *43*, 140–151.

(23) Frisch, M. J.; Trucks, G. W.; Schlegel, H. B.; Scuseria, G. E.; Robb, M. A.; Cheeseman, J. R.; Montgomery, J. A.; Vreven, T.; Kudin, K. N.; Burant, J. C.; Millam, J. M.; Iyengar, S. S.; Tomasi, J.; Barone, V.; Mennucci, B.; Cossi, M.; Scalmani, G.; Rega, N.; Petersson, G. A.; Nakatsuji, H.; Hada, M.; Ehara, M.; Toyota, K.; Fukuda, R.; Hasegawa, J.; Ishida, M.; Nakajima, T.; Honda, Y.; Kitao, O.; Nakai, H.; Klene, M.; Li, X.; Knox, J. E.; Hratchian, H. P.; Cross, J. B.; Adamo, C.; Jaramillo, J.; Gomperts, R.; Stratmann, R. E.; Yazyev, O.; Austin, A. J.; Cammi, R.; Pomelli, C.; Ochterski, J. W.; Ayala, P. Y.; Morokuma, K.; Voth, G. A.; Salvador, P.; Dannenberg, J. J.; Zakrzewski, V. G.; Dapprich, S.; Daniels, A. D.; Strain, M. C.; Farkas, O.; Malick, D. K.; Rabuck, A. D.; Raghavachari, K.; Foresman, J. B.; Ortiz, J. V.; Cui, Q.; Baboul, A. G.; Clifford, S.; Cioslowski, J.; Stefanov, B. B.; Liu, G.; Liashenko, A.; Piskorz,P.; Komaromi, I.; Martin, R. L.; Fox, D. J.; Keith, T.; Al-Laham, M. A.; Peng, C. Y.; Nanayakkara, A.; Challacombe, M.; Gill, P. M. W.;

Johnson, B.; Chen, W.; Wong, M. W.; Gonzalez, C.; Pople, J. A. *Gaussian03*, revision B.04; Gaussian, Inc.: Pittsburgh, PA, 2003.
(24) Schlegel, H. B. *J. Comput. Chem.* **1982**, *3*, 214.
(25) Peng, C.; Schlegel, H. B. *Isr. J. Chem.* **1994**, *33*, 449.
(26) Peng, C.; Ayala, P. Y.; Schlegel, H. B.; Frisch, M. J. *J. Comput. Chem.* **1996**, *17*, 49.
(27) Berente, I.; Naray-Szabo, G. *J. Phys. Chem. A* **2006**, *110*, 772–778.
(28) Gonzalez, C.; Schlegel, H. B. *J. Chem. Phys.* **1989**, *90*, 2154.
(29) Gonzalez, C.; Schlegel, H. B. *J. Phys. Chem.* **1990**, *94*, 5523.
(30) (a) Becke, A. D. *Phys. Rev. A* **1988**, *38*, 3098. (b) Becke, A. D. *J. Chem. Phys.* **1993**, *98*, 5648. (c) Lee, C.; Yang, W.; Parr, R. G. *Phys. Rev. B* **1988**, *37*, 785.
(31) Schafer, A.; Huber, C.; Ahlrichs, R. *J. Chem. Phys.* **1994**, *100*, 5829.
(32) Boys, S. F.; Bernardi, F. *Mol. Phys.* **1970**, *19*, 553.
(33) Simon, S.; Duran, M.; Dannenberg, J. J. *J. Chem. Phys.* **1996**, *105*, 11024.
(34) Dong, F.; Heinbuch, S.; Rocca, J. J.; Bernstein, E. R. To be published.
(35) Schröder, D.; Shaik, S.; Schwarz, H. *Acc. Chem. Res.* **2000**, *33*, 139.

JP7115774